



Quality Of Service and MObility driven cognitive radio Systems

White Paper

# Flexible Multicarrier PHY Design for Opportunistic Spectrum Access

## **ABSTRACT**

Opportunistic use of White Spaces (WS) has opened up a whole new paradigm in research on cognitive radio (CR). One of the issues addressed by the QoSMOS project is the design of a flexible and efficient physical layer (PHY) for CR systems. To this aim, different modulation techniques are being investigated and are presented in this paper. They fulfil the low out of band leakage and spectral efficiency requirements of a CR operating in fragmented WS. The design of reconfigurable and flexible radio-frequency (RF) front-end is also introduced, since its performance is tightly linked to these parameters and to the implementation feasibility and constraints. Emphasis is put on benchmarking the performance of the proposed schemes over classical approaches.

## INTRODUCTION

Recent regulations allowing opportunistic use of WS in licensed frequency bands has inspired numerous research activities on CR [1]. The European FP7 QoSMOS project [2] proposes to develop a framework for Quality of Service (QoS) and mobility driven CR systems in the WS. One key challenge for the opportunistic radio communication is the design of flexible PHY. QoSMOS aims at designing a robust PHY adapted to a heavily fragmented spectrum: the envisaged transmitted waveform should achieve high spectrum efficiency while meeting the constraints of a flexible RF architecture.

Multicarrier PHY are expected to meet these requirements and OFDM is the initial choice for any multicarrier systems, since it has been deployed prominently for many applications (cellular, WLAN, broadcast). Unfortunately OFDM shows strong spectral leakage in adjacent bands, whereas WS radio (eg. in TVWS) are ruled by stringent requirements on this parameter in order to protect adjacent incumbent systems. In order to fulfil QoSMOS requirements, where incumbent signals are not to be interfered with, innovative multicarrier modulation techniques should be proposed as alternative solutions for CR PHY design.

To improve spectrum efficiency, three modulation techniques are considered in QoSMOS: the Filter Bank Multi Carrier (FBMC) concept [3], the innovative Interference Avoidance transmission by Partitioned Frequency Time domain (IA-PFT) and the Generalized Frequency Division Multiplexing (GFDM) [4], with a reduced Cyclic Prefix. They aim at achieving low adjacent leakage spectrum, while maintaining or even increasing the high spectral efficiency of classical multicarrier schemes. These techniques appear to be good candidates for CR PHY. Further requirements and performance parameters are analysed and supported by simulations in the paper.

The other aspect addressed in this paper is that an efficient CR system requires spectrum aggregation capability and demands flexible RF architectures which complement the sophisticated baseband processing.

## Interference Avoidance Transmission by Windowing

Orthogonal Frequency Division Multiplexing (OFDM) is the favourite air-interface for cognitive radio systems, since by nulling some subcarriers we can easily shape the spectrum [15]. An OFDM signal is composed of a sum of many sinusoidal carriers modulated by the data symbols and windowed by a rectangular function. The application of a rectangular window in the time domain is equivalent to the spectral shaping by the sinc pulse [16]. This leads to a spectral spreading of the transmitted signal, causing interference to systems working at adjacent channels. The simplest and less complex technique to alleviate this problem is windowing. Although the achieved degree of sidelobe suppression is lower than the other methods [16] and since the signal is extended in time domain the resulting spectral efficiency is lower. A windowing technique in the time domain is used in IEEE802.11a [7].

### Transmitter Structure

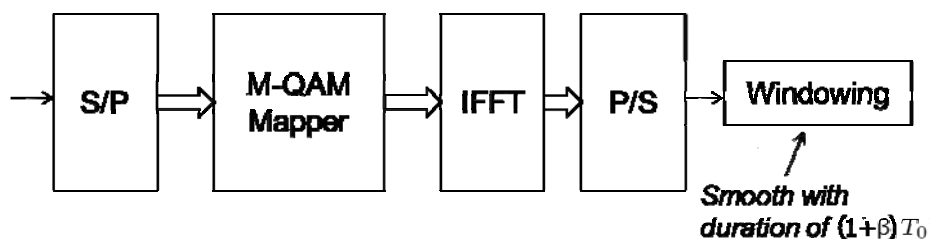


Figure 1. Transmitter structure for the windowing scheme.  $\beta$  denotes the window roll-off factor and  $T_0$  the symbol period length of conventional OFDM using a rectangular window.

In the windowing technique the transmitter structure is similar to the one of conventional OFDM, the only replacement being the windowing at the end of the chain, as shown in Figure 1. Hence, most of the transmitter blocks are reused, which is of course important for a smooth evolution.

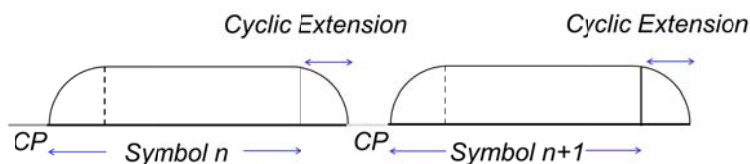


Figure 2. Windowed OFDM symbols in time domain.

The window block is comprised of two main sub-blocks. The first cyclically extends the incoming symbol and the second applies the window function and add an all zeros cyclic prefix (CP), as shown in Fig. 2.

The soft window is designed based on the characteristics of functions with vestigial symmetry which are common in baseband data transmission. By using the vestigial symmetry and requiring at the extremes of the window several null derivatives, it is possible to control a fast out-of-band decay. The proposed window (NP), with two null derivatives, is shown in Figure 3, where we also depict the raised cosine (RC) window for comparison purposes.

## Performance Windowing

Figure 4 presents an example of the transmission spectrum of the proposed window in comparison with conventional OFDM (rectangular window) and the raised cosine window. An FFT size of 1024 (the middle 512 are used for data transmission) and a subcarrier spacing of 15 kHz has been considered.

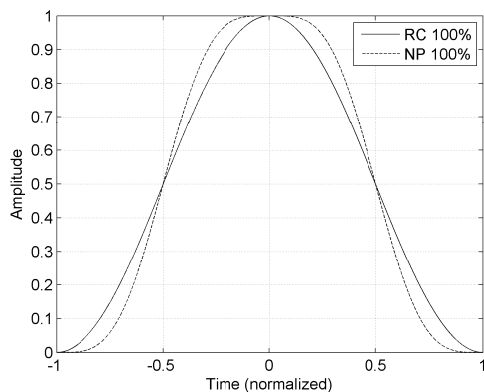


Figure 3. Comparison of the new pulse with raised cosine.

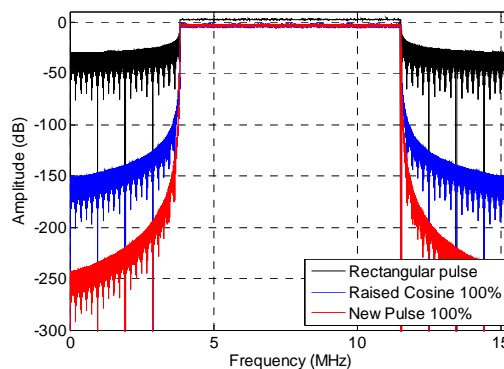


Figure 4. Power spectrum density for different windows.

There is a gain of around 90 dB between the raised cosine pulse and the new proposed pulse in the out of band region. Figure 5 shows results for the maximum transmit power an opportunistic user is allowed to transmit if a target BER of  $10^{-4}$  is to be respected at the incumbent. Both a Gaussian and a multipath channels are considered as well as different guard band intervals.

The proposed window has a similar performance to the raised cosine one, but with around 90% of overhead savings. Henceforth, due to its spectral leakage attenuation properties and low overhead the addition of the proposed window in the conventional OFDM systems allows a smooth evolution path for the introduction of the cognitive radio paradigm in the current wireless communication systems.

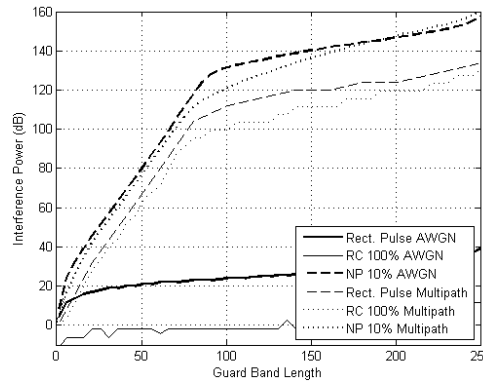


Figure 5. Interference Power versus Guard Band Length

## FBMC Physical Layer

In recent CR literature, filter bank based signal processing has been recognized as a high performance technique particularly well-suited for the opportunistic user transceiver [5]. The QoS MOS project is proposing a real-time validation of a CR system based on FBMC. For this purpose, a hardware test bed is being developed.

In this section, FBMC modulation is introduced and spectral efficiency gains are computed for different study cases.

The FBMC structure is described in Fig. 6. A transmultiplexer is the core of the system. The synthesis filter bank consists of all parallel transmit filters and the analysis filter bank includes the matching receive filters.

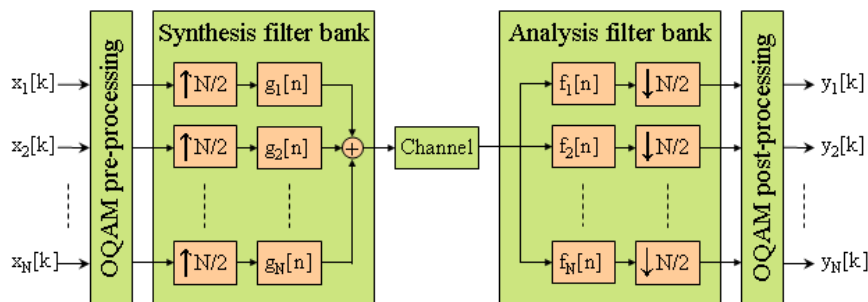
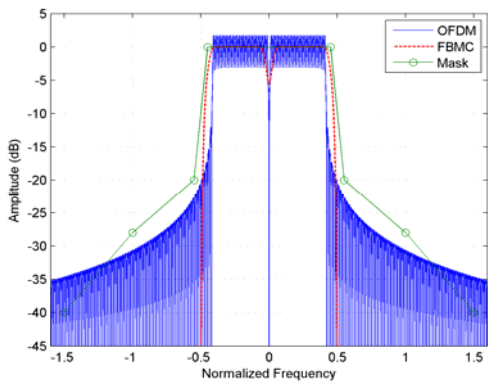


Figure 6. Structure of the FBMC modulation and demodulation.

The distinctive feature of the FBMC technique is its ability to provide improved frequency selectivity through spectrally well-shaped prototype filters at the cost of a longer impulse response. Due to the frequency selectivity of the channel, FBMC only requires orthogonality for the neighbouring sub-channels and offset quadrature amplitude modulation (OQAM) is used for this purpose. The combination of filter bank with OQAM modulation guarantees the orthogonality without the need of a CP as opposed to OFDM. Thus, the data rate loss induced by CP is avoided.

In comparison to OFDM architectures, FBMC introduces a complexity overhead that is not negligible. It is therefore essential to understand the spectral efficiency gain provided by FBMC techniques in comparison to OFDM. We propose to illustrate the potential spectral gain by using a practical approach based on two examples inspired by widely deployed standards: DVB-T and IEEE 802.11a/g. In both examples, the gain in terms of number of frequency carriers will be first estimated assuming the spectrum mask recommended in the standard. This gain will be called the frequency gain. The gain coming from the absence of CP will then be estimated and will be called time gain. Both gains will be added to estimate the overall spectral efficiency gain.



*Extremely low out of band leakage for FBMC makes it suitable for cognitive radio usage in fragmented spectrum*

Figure 7. Power spectral density comparison in IEEE 802.11a/g.

FBMC has shown strong spectral efficiency performance. The results should further favour FBMC for applications where out of band radiation power levels are critical. This is particularly the case of CR communication systems. For instance, the FCC requests that adjacent leakage should be 55dB lower than the in-band signal.

Due to multipath propagation, equalization has to be performed. In conventional multicarrier systems the most common technique is the CP based approach because of its robustness and simplicity. The use of the CP mitigates the Inter-Symbol Interference (ISI) as long as the CP is longer than the channel delay spread. Only linear distortions will appear during equalization, which can be compensated by a phase and amplitude correction.

The absence of a CP in FBMC inevitably leads to ISI which causes an error floor to appear for high SNR regimes. Several approaches have been proposed for the equalization of FBMC systems such as in [17][18]. These methods are based on a per subcarrier MMSE equalization. Simulation results are shown in Fig. 8.

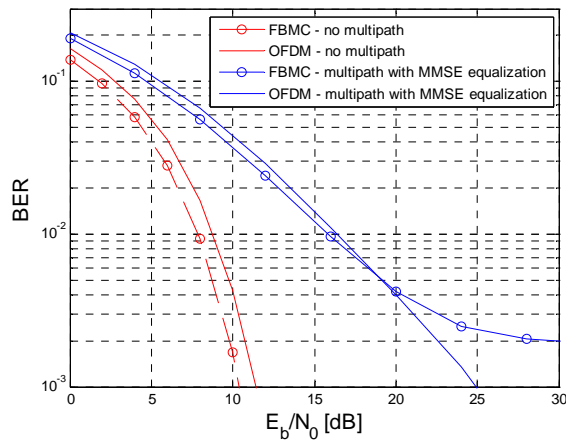


Figure 8. BER versus  $E_b/N_0$  for the FBMC and OFDM MMSE equalization schemes over AWGN and multipath channels.

It can be seen that for the AWGN channel the FBMC system outperforms the OFDM system with CP. The Bit Error Rate (BER) values for FMBC over multipath channels using equalization for SNR values lower than 20 dB are still slightly better. On the other hand, when reaching higher SNR values, the FBMC system exhibits an error floor due to the residual ISI, regardless of the chosen equalization technique. This phenomenon will be mitigated when error correction coding is applied.

To enable better detection, an iterative decision feedback equalization technique was also proposed, but eventually this scheme also reaches an error floor. This relatively low error floor can be mitigated by appropriate coding. Hence, FBMC is a viable alternative to OFDM demanding moderate complexity increase in the equalizer.

Apart from channel equalization the large Peak-to-Average Power (PAPR) of the signal will be also an important issue, due to the fact that if nonlinearities are present in the transceiver chain, the ACLR may significantly rise. The FBMC signal itself has a similar amplitude distribution as OFDM due to the fact that the modulated signal is the sum of numerous independently modulated subcarriers. In order to address this phenomenon PAPR reduction techniques suitable to FBMC were developed in Qosmos [18].

## Interference Avoidance Transmission by IA-PFT

Aiming at reducing the undesired spectrum emission caused by the opportunistic system, the new method IA-PFT is proposed. The following sub-sections present an overview and fundamental performances of IA-PFT.

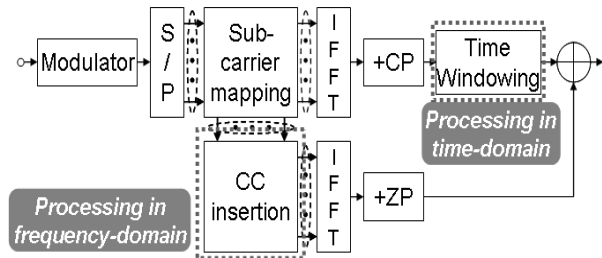


Figure 9. IA-PFT transmitter structure.

### IA-PFT Transmitter Structure

IA-PFT structure features a parallel combination scheme of Time Windowing (TW) [7] and Cancellation Carrier (CC) [11][12] as shown in Fig. 9. The transmitted bit stream is modulated and divided into a signal group to be processed by TW and a signal group to be processed by CC at the subcarrier mapping block. TW processed signal group is converted by IFFT. Then, a CP is appended to the head of the OFDM symbols. After appending CP, signal shaping in time-domain is carried out at the TW block. On the other hand, CC processed signal group is fed to CC insertion block. At CC insertion block, CC vector is inserted to CC processed signal group in frequency-domain to suppress the undesired spectrum emission in interference avoidance band. After converting by IFFT, a Zero-Padding (ZP) guard interval is appended to the head of the OFDM symbols. Finally, TW processed signal group and CC processed signal group are multiplexed.

### Interference Suppression Performance

Fig. 10 shows a comparison example of transmission spectrum of the interference avoidance transmission techniques, where the major parameters listed in Table I is assumed. The number of interference avoidance band ( $N_i$ ) is equivalent to 32 turned off sub-carriers. IA-PFT is applied to each spectrum edge (two CC at each spectrum edge). According to the simulation result, TW alone cannot achieve the high suppression gain near the transmission subcarriers in the interference avoidance band. Meanwhile, CC alone cannot achieve the high suppression gain near the centre of the interference avoidance band. For IA-PFT, the maximum suppression gains of power spectrum density are respectively 6 dB and 12 dB better than those of CC and TW.

Fig. 11 shows the power spectrum density of IA-PFT when a parameter  $Q$  is changed. The parameter  $Q$  represents the number of subcarriers being processed by CC insertion block per spectrum edge. In other words, the allocation ratio between TW processed signal and CC processed signal can be determined by  $Q$ . As seen from the evaluation results in Fig. 11, if  $Q$  is set to a small value, the power spectrum density of IA-PFT approaches that of TW. If  $Q$  is set to a large value, the power spectrum density of IA-PFT approaches that of CC.



TABLE I. SIMULATION PARAMETERS.

Parameter	Assumption
FFT size	1024
Maximum number of subcarriers	600
CP (ZP) sample	72
Subcarrier spacing	15 kHz
Modulation	QPSK

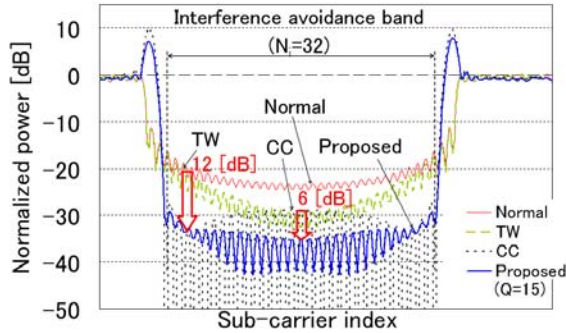


Figure 10. Power spectrum density of IA-PFT.

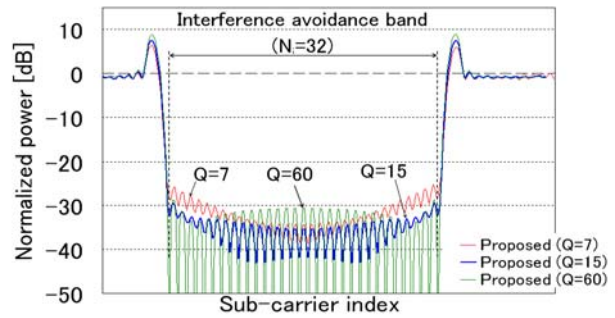


Figure 11. Power spectrum density of IA-PFT with variable  $Q$ .

## Evaluation of PAPR

Fig. 12 shows Peak to Average Power Ratio (PAPR) of IA-PFT transmission signals. In this evaluation, the simulation parameters were set to the same values as in Fig. 10.

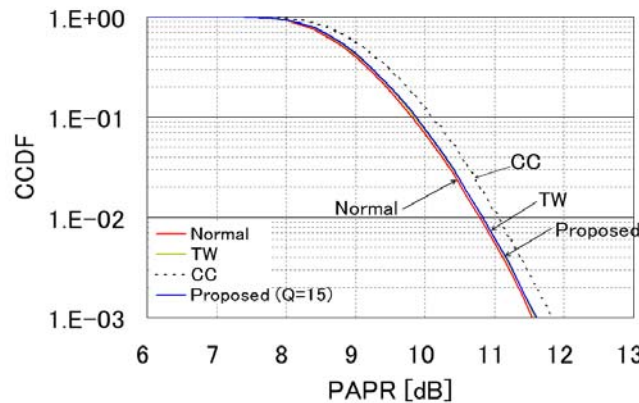


Figure 12. PAPR performance of IA-PFT.

According to the simulation result, PAPR of CC is increased by 0.3 dB compared to a normal OFDM when Complementary Cumulative Distribution Function (CCDF) is equivalent to 1%. It can be seen that the increase of PAPR for CC is caused by ZP used for all the subcarriers instead of CP. On the other hand, PAPR of IA-PFT is almost same as that of the normal OFDM since ZP is partially used for the subcarriers.

It is therefore concluded that IA-PFT is a promising candidate for QoS MOS transmitter. It is also noted that typical OFDM receivers can be applied for IA-PFT.

## General Frequency Division Multiplex

GFDM [4] is a new multicarrier modulation technique which is particularly suitable for cognitive PHY in fragmented white spaces. Not being restricted to rectangular pulse, as in

OFDM, here in GFDM, the choice of suitable Nyquist pulse shape restricts the out of band radiation of the opportunistic signals to interfere with the incumbent.

GFDM is a multicarrier system incorporating a tail-biting technique. The transmit signal block has a CP accounting for the Tx/Rx filtering and the mobile channel. The CP is shortened by dropping the Tx/Rx filter part [11] and then the tail of the payload is added onto the CP to emulate circular convolution. In the transmitter part of the system, as shown in Fig. 13, the binary data is QAM modulated and then the transmit pulse shaping filter shapes the modulated data, to improve spectral efficiency. Then after up-conversion the transmitter transmits the modulated signals with CP.

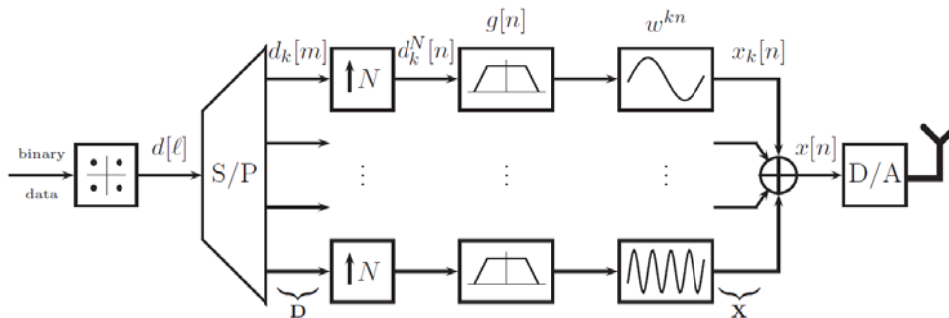


Figure 13. GFDM transmit system model.

In the receiver part of the system, as shown in Fig. 14, the CP is removed and then after equalization, down conversion is performed. The received signal is then passed through the matched received pulse shaping filter, followed by a sampler and a detector to get back the binary data.

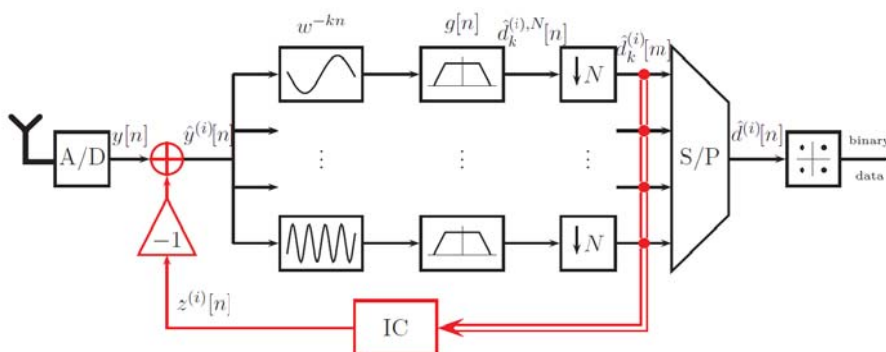


Figure 14. GFDM receive system model.

As shown in [4], the PAPR of this system is better than that of OFDM by about 1 dB at 1% CCDF; as here we have less number of subcarriers compared to OFDM. The tail-biting technique, even though increases the throughput of the system, causes Inter-Carrier Interference (ICI) between two adjacent subcarriers, not only at the same time instant, but also with symbols with different time stamp. Because of non-orthogonality of the subcarriers, ICI is very pronounced and, as shown in Fig. 15, the BER curve of GFDM is a bit degraded compared to theoretical AWGN BER curve. Using a successive interference cancellation, GFDM could achieve good performance, demanding reasonable complexity increase in the equalizer.

GFDM shows a lot of potential for being adopted as a multicarrier modulation technique in CR PHY design. The choice of pulse shaping techniques makes the spectral mask highly efficient and hence is a suitable candidate for adaptation in QoS-MOS PHY design



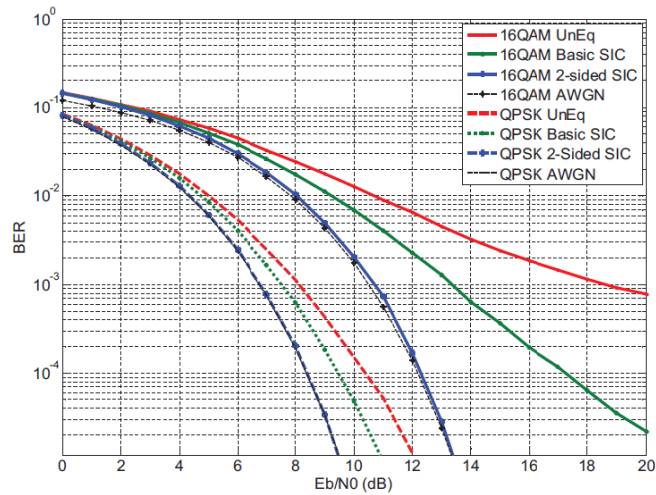


Figure 15. BER performance of GFDM vs theoretical AWGN BER.

## RECONFIGURABLE RF TRANSCEIVER FRONT-END (FE)

Cognitive radio (CR) RFFEs are supposed to cover multiple frequency bands to allow opportunistic and dynamic usage of spectral white spaces. Therefore, the RF section needs to be particularly flexible. The key building block for these reconfigurable RFFEs is the RF tuneable band pass filter (t-BPF) for image rejection purposes. While other components (e.g. broadband mixer, wide frequency range local oscillators) are off-the-shelf components, digitally tuneable RF BPF are hardly available on the market. Since the digitally tuneable RF BPFs are considered to be the key components of the reconfigurable RFFE [15], a digitally t-BPF and tuneable low pass filter (t-LPF) was designed in QoSMOS project [16]. In addition, CR transceiver RFFEs should have a good performance (e.g. selectivity, sensitivity, linearity).

The PHY layer hardware concept is portrayed in Figure 16. It consists of several modules: the baseband board, the RF transmitter FE, and up to two RF receiver FEs. The digital signal processing as well as the hardware (re)configuration is performed by the baseband board, which includes an FPGA, an analogue-to-digital converter (ADC), and a digital-to-analogue converter (DAC). The analogue signal processing is performed by the RFFE boards. This includes the frequency conversion, amplification, and filtering of the received signals and the signals to be transmitted, respectively.

In the following sections, a general view on the hardware concept and the requirements are given, which led to the concept selected.

### RF Transceiver Front-End requirement

The requirements on the reconfigurable RFFE for CR in QoSMOS project are:

- to cover the frequency range from 470 MHz to 860 MHz
- to be able to handle signal bandwidth from 8 MHz up to 40 MHz
- to deliver a maximal output power of +17 dBm
- to have an input range from -3 dBm down to -90 dBm
- to have an ALCR better than 55 dB

In the following subsection, the RFFE architecture is proposed that consist of a reconfigurable RF part.

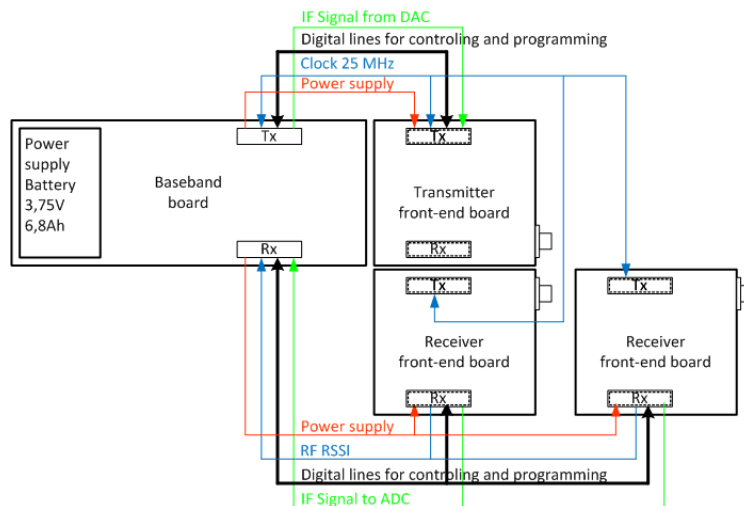


Figure 16: Schematic view of the hardware concept consisting of a baseband board, a transmitter front-end, and two receiver front-ends

## RF Transceiver Front-End Implementation

Figure 17 and Figure 18 portray the proposed architecture of the reconfigurable RF transmitter and receiver FE respectively. The architecture is based on the use of super heterodyne architecture and offers only one down-converting stage. The bandwidth of the transmitter and the receiver FE is given by the IF BPF which offers a 40 MHz nominal bandwidth. Of course, the tuneable BPF on RF section also support this bandwidth. As RF is supposed to be tuneable over a wide frequency range, the t-BPF has to be adjusted to the respective channel during operation in accordance with the present situation. As seen in Figure 17 and Figure 18, three components are reconfigurable in terms of frequency band: the t-LPF, the t-BPF and the LO. These components are programmable via a 3-wire serial bus interface.

The RF transmitter FE is composed by the following building blocks: IF BPF, broadband RF/IF amplifier, broadband mixer, t-BPF and t-LPF, digital variable attenuator (DVA), local oscillator (LO) and power amplifier (PA).

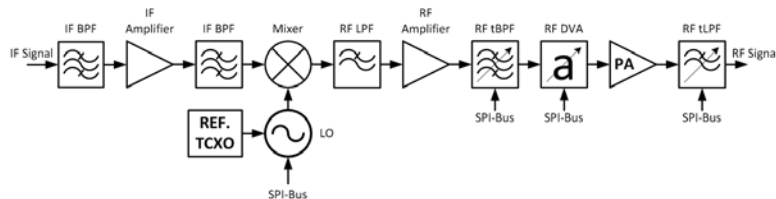


Figure 17: Reconfigurable RF Transmitter FE architecture

The IF-Signal generated by the DAC is filtered, amplified and filtered to suppress the out-of-band spurious signals and higher-order harmonics generated by the DAC. By means of a programmable phase-locked loop (PLL) device which serves as LO the RF signal can be arbitrarily positioned within the frequency region of interest. After up-conversion the RF signal is filtered and amplified by LPF, t-BPF and RF amplifier. The filters suppress undesired mixing products. Further it passes the DVA that allows adjusting the output signal level for different frequency bands. The RF BPF signal is amplified by the PA to have the maximal output power. The t-LPF at the output is used to suppress spurious signals and higher-order harmonics caused by the PA. The key characteristics of the RF transmitter FE are given in Table 2.

Parameter	specification	Condition
RF Frequency range	470 MHz to 860 MHz	
Gain	ca. 16 dB	
Output IP3	30 dBm	2 tone output level@+10 dBm
SFDR	70 dB	In 40 MHz band
Bandwidth	40 MHz	
Max. Output power	+17 dBm	
Dynamic range	31 dB	In 0.25 dB steps

Table 2: The key parameters of the RF transmitter Front-end

The RF receiver is composed by the following building blocks: t-LPF and t-BPF, low noise amplifier (LNA), DVA, IF amplifier, broadband mixer, IF LPF and BPF, LO and power detector.

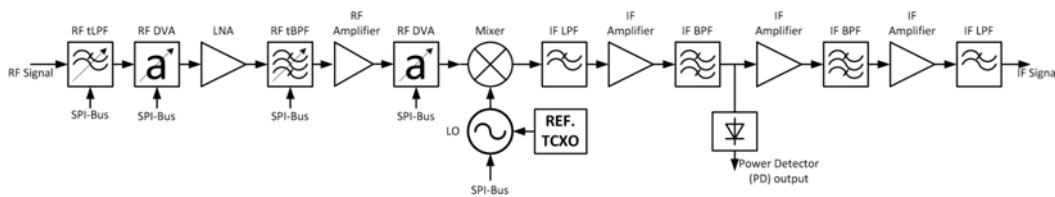


Figure 18: Reconfigurable RF receiver FE architecture

The RF signal received by antenna is first filtered by a t-LPF that suppresses out-of-band signals and images. Further it passes the DVA that helps to prevent overload and distortion. The signal is then amplified by a LNA, which suppresses the contribution of the noise from the succeeding stages. The LNA output is filtered by a t-BPF that serves as pre-selection filter. The band-limited signal passes another low-noise amplifier and DVA, the latter allowing to adjust the signal level appropriately. The signal is then down-converted to the IF. The IF signal is filtered and amplified by two IF BPF and LPF, all serving as anti-aliasing filters (AAF), before it is fed to an ADC. The design contains an external power detector that provides an analogue voltage measure in order to monitor the received power with the baseband board. The key characteristics of the RF receiver FE are given in Table 3.

Parameter	specification	Condition
RF Frequency range	470 MHz to 860 MHz	
Bandwidth	40 MHz	
Gain	ca. 35 dB	With 0 dBm at the output
Input IP3	-7 dBm	2 tone output level@ 0 dBm
SFDR	75 dB	0 dBFS at ADC
AGC Adjustment range	31 dB	In 0.25 dB steps
Noise Figure	< 4 dB	Max. Gain
Dynamic range	87 dB	
Sensitivity	-90 dBm	10 dB SNR with modulated signal of 8 MHz BW

Table 3: The key parameters of the RF receiver Front-end

## Acknowledgment

This work has been performed in the framework of the EC funded project QoS MOS, FP7-ICT-2009/248454.

## AUTHORS

Vincent Berg (vincent.berg[at]cea.fr) – CEA-LETI, France.  
Dominique Noguét (dominique.noguét[at]cea.fr) – CEA-LETI, France.  
Yasunori Futatsugi (y-futatsugi[at]cq.jp.nec.com) – NEC, Japan.  
Masayuki Ariyoshi (ariyoshi[at]bx.jp.nec.com) – NEC, Japan.  
Mario Schühler (mario.schuehler[at]iis.fraunhofer.de) – Fraunhofer IIS, Germany.  
Mengistu Tessema (mengistu.tessema@iis.fraunhofer.de) – Fraunhofer IIS, Germany.  
Zsolt Kollar (kollar[at]mht.bme.hu) – BME, Hungary.  
Peter Horvath (hp[at]mht.bme.hu) - BME, Hungary.  
Péter Bakki (bakki[at]mht.bme.hu) - BME, Hungary.  
Atilio Gameiro (amg[at]ua.pt) – IT, Portugal.  
Daniel Castanheira (dcastanheira[at]av.it.pt) – IT, Portugal.  
Rohit Datta (rohit.datta[at]ifn.et.tu-dresden.de) –TU Dresden, Germany.  
Gerhard Fettweis (fettweis[at]ifn.et.tu-dresden.de) – TU Dresden, Germany.

## REFERENCES

- [1] J. Mitola, "Cognitive radio: an integrated agent architecture for software defined radio", Ph.D. thesis, Royal Institute of Technology, Stockholm, Sweden, May 2000.
- [2] QoS MOS project website. available at: <http://www.ict-qosmos.eu>
- [3] P. Siohan, C. Siclet and N. Lacaille, "Analysis and design of OFDM/OQAM systems based on filterbank theory", IEEE Transactions on Signal Processing, vol.50, no.5, pp.1170-1183, May 2002.
- [4] G. Fettweis, M. Krondorf and S. Bittner, "GFDM – General Frequency Division Multiplexing", in Proceedings of IEEE 69th Vehicular Technology Conference (VTC Spring'09), 26-29 April 2009.
- [5] H. Zhang, D. Le Ruyet and M. Terre, "Spectral Efficiency Analysis in OFDM and OFDM/OQAM Based Cognitive Radio Networks", in Proceedings of IEEE 69th Vehicular Technology Conference (VTC Spring'09), 26-29 April 2009.
- [6] ETSI EN 300 744 V1.6.1 (2009-01). Digital Video Broadcasting (DVB), Framing Structure, Channel Coding and Modulation for Digital Terrestrial Television. European Standard ETSI, 2009.
- [7] IEEE, "Supplement to IEEE Standard for Information technology—Telecommunications and information exchange between systems—Local and metropolitan area networks—Specific requirements—Part 11: Wireless LAN Medium Access Control (MAC) and Physical Layer (PHY) specifications: High-speed Physical Layer in the 5 GHz Band," IEEE Std 802.11a-1999.
- [8] A. Ikhlef and J. Louveaux, "An enhanced MMSE per subchannel equalizer for highly frequency selective channels for FBMC/OQAM systems", in Proceedings of IEEE Signal Processing Advances in Wireless Communications (SPAWC'09), June 2009.
- [9] T. Ihalainen, T. H. Stitz, and M. Renfors, "Efficient per-carrier channel equalizer for filter bank based multicarrier systems", in Proceedings of IEEE International Symposium on Circuits and Systems (ISCAS '05), May 2005, pp. 3175–3178.
- [10] Zs. Kollár, G. Péceli and P. Horváth, "Iterative decision feedback equalization for FBMC systems", in Proceedings of IEEE First International Conference on Advances in Cognitive Radio, (COCORA 2011), April 2011.
- [11] H. Yamaguchi, "Active interference cancellation technique for MB-OFDM cognitive radio", Microwave conference 2004, pp.1105–1108, Oct. 2004.
- [12] S. Brandes, I. Cosovic and M. Schnell, "Sidelobe suppression in OFDM systems by insertion of cancellation carriers", VTC2005-Fall, pp.152–156, Sept. 2005.
- [13] N. Michailow, M. Lentmaier, P. Rost and G. Fettweis, "Integration of a GFDM Secondary System in an OFDM Primary System", accepted for publication in FuNeMs 2011, Warsaw, Poland.
- [14] B. Razavi, "RF transmitter architectures and circuits", in Proceedings of the IEEE 1999 Custom Integrated Circuits, San Diego, CA, May 16-19, 1999, pp. 197-204.

- [15] Marey, M.; Dobre, O.; Willink, T.; , "A new algorithm for sidelobe suppression and performance comparison in DFT-OFDM cognitive radios," Signals, Systems and Computers (ASILOMAR), 2010 Conference Record of the Forty Fourth Asilomar Conference on , vol., no., pp.441-445, 7-10 Nov. 2010
- [16] J. Luo, W. Keusgen, and A. Kortke, Optimization of time domain windowing and guardband size for cellular OFDM systems, in Proc. IEEE VTC-Fall, Sep. 2008.
- [17] Y. Dandach and P. Siohan. "FBMC/OQAM modulators with half complexity". 2011 IEEE, Global Telecommunications Conference (GLOBECOM 2011), pages 1-5, December 2011.
- [18] Zs. Kollár, L. Varga, and K. Czimer. Clipping-based iterative PAPR-reduction techniques for FBMC. In OFDM-Workshop 2012, InOWo'12, pages 139145, August 2012. paper OFDM12-10.
- [19] D. Castanheira and A. Gameiro, Novel Windowing Scheme for Cognitive OFDM Systems, Accepted for publication in the IEEE Communication Letters